文章编号:1001-9014(2007)03-0161-03

# BROAD-BAND TRIPLER OF W-BAND

YANG Tao[1], XIANG Zhi-Jun[2], WU Wei[1], YANG Zi-Qiang[1], QIAN Ke-Wei[1]
(1. Microwave Center, University of Electronic Science and Technology of China, Chengdu 610054, China;
2. Southwest Institute of Electronic Equipment of China (SWIEE), Chengdu 610054, China)

**Abstract**: A W-band broadband frequency tripler was formed by anti-parallel Schottky-barrier diode pair. The input signal was fed in by a WR-28 waveguide-to-microstrip transition, and the output signal was fed out by a reduced-height WR-10 waveguide. For the input power of 5dBm, the output power was 0.81 ± 1.80dBm and the second harmonic rejection was greater than 25dBc in the whole W-band. This tripler can be used to extend Ka-band signal source to W-band.
**Key words**: W-band tripler; balanced circuit; Schottky-barrier diode
**CLC number**: TN45 **Document**: A

# W频段宽带倍频器

杨 涛[1], 向志军[2], 吴 伟[1], 杨自强[1], 钱可伟[1]
(1. 电子科技大学 微波中心, 四川 成都 610054; 2. 西南电子设备研究所, 四川 成都 610054)

**摘要**:介绍了一个W频段宽带倍频器.采用反向并联二极管对结构实现宽带倍频.该倍频器输入为WR-28波导到微带过渡结构,输出为WR-10减高波导.在输入功率为5dBm时,在整个W频段输出功率为0.81±1.80dBm,二次谐波抑制度大于25dBc.该倍频器可把Ka频段的信号源扩展到W频段.
**关 键 词**:W频段倍频器;平衡电路;肖特基势垒二极管

## Introduction

Frequency multiplier is widely used in millimeter-wave signal sources and transceivers. It can be used to extend the frequency range of microwave signal sources up to millimeter-wave band while maintaining the performances of the microwave signal sources, such as high stability and low phase noise [1]. In order to cover a full waveguide bandwidth, Schottky-barrier diodes are used to achieve broad band resistive frequency multipliers [2]. W-band signal source is widely used in communication, radar, guided missile and so on[3]. The input signal of 25 ~ 36.7GHz can be extended to 75 ~ 110GHz by a frequency multiplier and amplifier module.

## 1 Theory of tripler

The anti-parallel balanced circuit is shown in Figure1. These two diodes present anti-parallel as to input and output circuits[4].

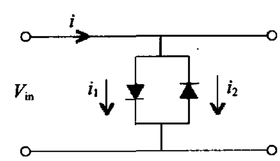


Fig. 1 The balanced frequency tripler circuit
图1 平衡式倍频电路

The current-voltage (I/V) characteristic of the Schottky barrier junction is

$$i_1 = i_s[e^{\alpha V_{in}} - 1] \quad , \tag{1}$$

$$i_2 = -i_s[e^{-\alpha V_{in}} - 1] \quad , \tag{2}$$

where $i_s$ is the reversed saturation current; $\alpha = \frac{q}{nkT}$, where n is the ideality factor, a parameter that accounts for the junction non-ideality. Henceforth, the

**Received date**: 2006-12-22, **revised date**: 2007-03-07　　**收稿日期**:2006-12-22, **修回日期**:2007-03-07
**Foudantion Item**: The project is supported in part by the National Natural Science Foundation of China(60501012)
**Biography**: Yang Tao (1970-), male, Sichuan, China, associate professor. Research field is microwave and millimeter-wave circuit and system.

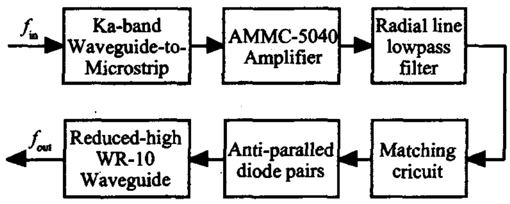


Fig. 2 W-band tripler architecture
图2 W频段倍频器组成

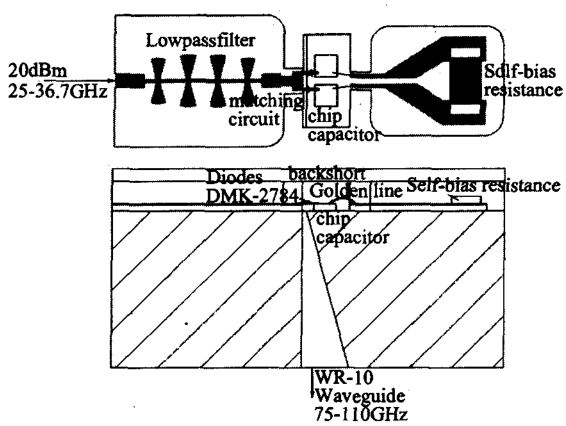


Fig. 3 W-band tripler structure
图3 W频段倍频器结构

input current can be derived as:

$$i_{in} = i_1 - i_2 = 2i_s\cosh(\alpha V_{in} - 1) \quad . \qquad (3)$$

Substituting $V_{in} = V_s\cos(\omega_s t)$ into (3), we get

$$i_{in} = i_1 - i_2 = 2i_s\cosh[\alpha V_s\cos(\omega_s t) - 1] \quad , \qquad (4)$$

where $\omega_s$ is the input frequency.

Applying series expansion to (4)

$$i_{in} = i_s[2I_0(\alpha V_s) - 2] + 4i_s[I_2(\alpha V_s)\cos 2\omega_s t + I_4(\alpha V_s)\cos 4\omega_s t + \cdots] \quad , \qquad (5)$$

where $I_n$ is the first kind modified Bessel fuction.

Now, equation (5) implies that the total input current contains only even harmonics of the input frequency.

Meanwhile, the output current can be obtained as:

$$i_{out} = i_1 + i_2 = 2i_s\sinh(\alpha V_{in}) \quad . \qquad (6)$$

Substituting $V_{in} = V_s\cos(\omega_s t)$ into (6), we get

$$i_{out} = 4i_s[I_1(\alpha V_s)\cos\omega_s t + I_3(\alpha V_s)\cos 3\omega_s t + \cdots] \quad , \qquad (7)$$

Equation (7) implies that the total output current contains only the fundamental and odd harmonics. The even harmonics rejection depends on the uniformity of the diodes and the symmetry of the circuits[5].

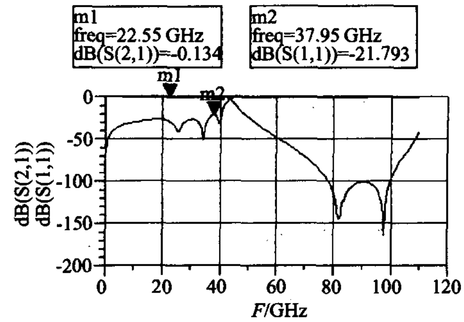


Fig. 4 The simulated results of lowpass filter
图4 低通滤波器仿真结果

## 2 Circuit design

The architecture of the tripler is shown in Fig. 2. The input signal is fed in by a WR-28 waveguide-to-microstrip transition. Then the signal is amplified by Agilent's AMMC-5040 MMIC amplifier with about 20dBm output power. The radial line lowpass filter is used to prevent third harmonics from returning to input circuit. The tripler circuit can be seen in Fig. 3. Diodes' two sides are laid on the microstrip line and chip capacitors respectively. The third harmonics is fed out by a reduced-height WR-10 waveguide, the rectilinear way is employed in this reduced-height waveguide to standard WR-10 waveguide transition because of its simple structure which is suitable for project application[7]. Self-biasing circuit is composed of chip capacitors and a self-biasing resistance.

Compared with conventional microstrip quarter wavelength open resonant line, the radial line has the following advantages [6,7]:

1. When low resistance resonant line is needed, the width of microstrip resonant line is increased, which possibly leads to unexpected influence on the lowpass filter. Whereas the radial line's input can be made smaller, and its resonant performance will not be influenced.

2. For the same resonant frequency, the radial line's length is shorter than the conventional microstrip resonant line.

3. The radial line has broader 3dB bandwidth when it is used as resonant line.

The radial line lowpass filter was optimized by Agilent's ADS Momentum, a commercially available 2.5D

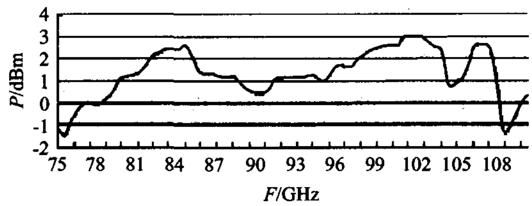


Fig. 5 Measured output power
图 5 输出功率测试结果

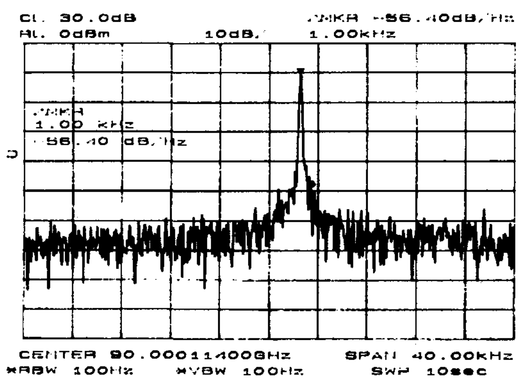


Fig. 6 Measured spectrum at 90GHz
图 6 90GHz 频谱图测试结果

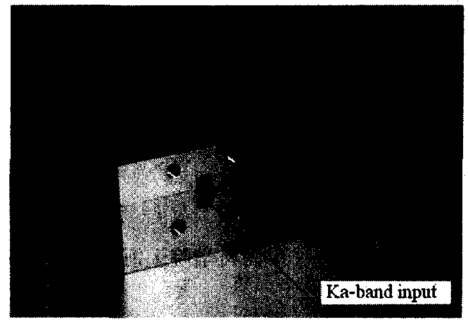


Fig. 7 W-28 waveguide input port
图 7 倍频器 W-28 波导输入口

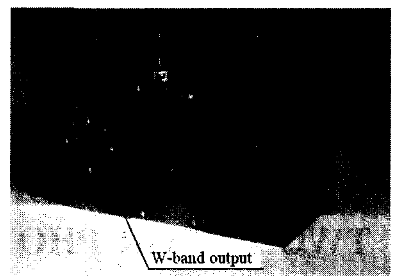


Fig. 8 W-10 waveguide output port
图 8 倍频器 W-10 波导输出口

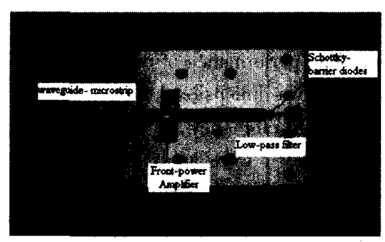


Fig. 9 Inside of the tripler
图 9 倍频器内部结构

method-of-moments simulator. The results are shown in Fig4.

The W-band tripler is simulated by using the harmonic balance simulator based on diode' s spice parameters. The optimal length of the b side of output reduced-height WR-10 waveguide is obtained by load pull simulation. Meanwhile, the input matching circuit is established by optimization.

## 3 Measured results

The measured output power of the tripler is shown in Fig. 5. As mentioned above, the input Ka-band signal is amplified to about 20dBm, the corresponding output power is 0. 81 ± 1. 80dBm in the whole W-band, which shows an excellent broad band performance. The input return loss is greater than 10dB. The output spectrum of the tripler is measured by a microwave spectrum analyzer and a harmonic mixer[8]. The second harmonic rejection is greater than 25dBc in the whole band. The measured output spectrum at 90GHz is shown in Fig. 6. The photograph of the tripler is shown in Fig. 7, Fig. 8 and Fig. 9.

## 4 Conclusion

A W-band tripler with compact structure and broadband performance is presented. It can be used to extend the Ka-band signals to W-band. Furthermore, by connecting a Ka-band doubler to this W-band tripler, an input signal of 12.5 ~ 18.3GHz can be extended to W-band.

## REFERENCES

[1] Zhang Yonghong, Tang Xiaohong, Feng Zhenghe. The investigation of W-band solid-state frequency sources[C]. *Microwave and Millimeter Wave Technology, Proceedings.* ICMMT 2002. 2002 3rd International Conference. 2002, 1125—1128.

[2] Maas S A, Ryu Y. A broadband planar monolithic resistive frequency doubler[J]. *IEEE MTT-S Digest*, 1994, 443—446.

(下转 186 页)

叶片红外热影像温度的回归直线相当接近,回归直线的斜率差异仅1%,代表红外热像仪发射率设定功能于微小温差环境±0.5℃并没有发挥效用.但红外热像仪发射率参数设定值与混凝土结构物、叶片红外热像平均温度标准误差的回归直线则有明显不同,两种目标物平均温度标准误差之回归直线的斜率差异达13%.

## REFERENCES

[1] SHAN Yong, ZHANG Jing-Zhou, LI Li-Guo. Numerical calculation and experimental verification for the infrared radiation characteristics of helicopter infrared radiation suppressor [J]. *J. Infrared Millim. Waves* (单勇,张靖周,李立国. 直升机红外抑制器红外辐射特性的数值研究和实验验证. **红外与毫米波学报**),2006,**25**(2):95—100.

[2] Avdelidis N P, Moropoulou A. Emissivity considerations in building thermography [J]. *Energy and Buildings*, 2003, **35**:663—667.

[3] Syed A R, Nasser M N. Fusion of FLIR automatic target recognition algorithms [J]. *Information Fusion*, 2003, **4**: 247—258.

[4] Lincoln T, Eduardo Z. *Plant Physiology* [M]. Massachusetts: Sinauer Associates Publisher, 1998.

[5] Mills A F. *Heat Transfer* [M]. Massachusetts: Irwin Publisher, 1992.

[6] Jacquemoud S, Baret F. PROSPECT: a model of leaf optical properties spectra [J]. *Remote Sens. Environ.*, 1990, **34**:75—91.

[7] Hopkins W G. *Introduction to Plant Physiology* [M]. New York: John Wiley Publisher, 1997.

[8] Yunus A G. *Introduction to Thermodynamics and Heat Transfer* [M]. New York: McGraw-Hill Press, 1997.

[9] Ri Quang Yi. *Infrared thermal measurement and remote sensing technique* [M]. Taiwan: Fu Han Publisher(依日光. **红外线遥感测热法**. 台湾:复汉出版社),1996.

(上接163页)

[3] LI Jun-Ming, ZHANG Zu-Yin, GUO Wei. Comparison of 3 mm and 8 mm waveband passive detection [J]. *J. Infrared Millim. Waves* (李俊明, 张祖荫, 郭伟. 3mm与8mm波段无源探测特性的比较. **红外与毫米波学报**), 2006, **25** (5):71—74.

[4] Stephen A Mass. *Nonlinear Microwave and RF Circuits* [M]. 2nd ed. Artech House, INC. 2003, 301—315.

[5] GAN Ti-Guo. Schottky diode applications in mm-wave integrated circuits [J]. *Telecommunication Engineering* (甘体国. 肖特基势垒二极管在毫米波集成电路中的应用. **电讯技术**), 1994, **34**(5):12—17.

[6] Atwater H A. The Design of the Radial Line Stub: A Useful Microstrip Circuit Element [J]. *Microwave Journal*, 1985, 149—156.

[7] Franco Giannini, Roberto Sorrentino, Jan Vrba. Planar circuit analysis of microstrip radial stub [J]. *IEEE MTT-S Digest*, 1984, 124—125.

[8] SHEN Xiao-Fang, YAO Qi-Jun, LIN Zhen-Hui, *et al.* Measurement of the frequency spectrum of a submillimeter CW source by heterodyne mixing and direct detection [J]. *J. Infrared Millim. Waves* (申小芳,姚骑均,林镇辉,等. 用外差混频和直接检波方法测量亚毫米波连续波源的频谱. **红外与毫米波学报**), 2005, **24**(5):321—327.